Lycium barbarum glycopeptide (wolfberry extract) slows N-methyl-N-nitrosourea-induced degradation of photoreceptors

Qihang Kong[1, 2, #], Xiu Han[3, #], Haiyang Cheng[3], Jiayu Liu[2], Huijun Zhang[2, 4], Tangrong Dong[5], Jiansu Chen[1, 6], Kwok-Fai So[3, 6, 7, 8], Xuesong Mi[2, 6, *], Ying Xu[3, 6, 7, *], Shibo Tang[1, 6, *]

From the Contents

Graphical Abstract

Lycium barbarum glycopeptide (LbGP) delays photoreceptor degeneration
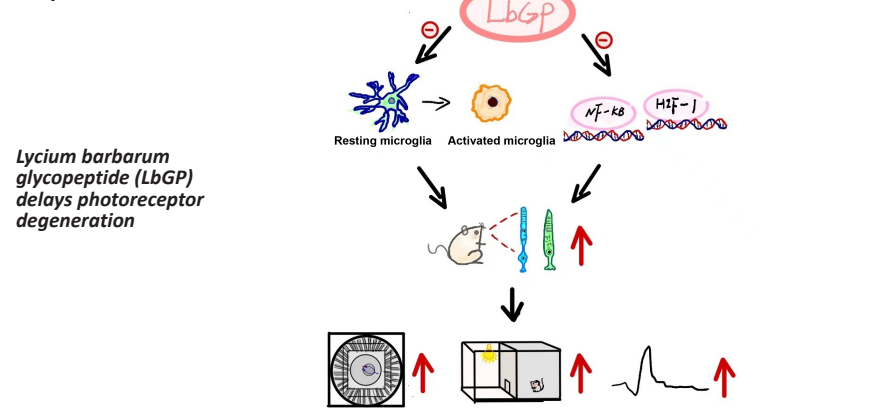
Abstract

Photoreceptor cell degeneration leads to blindness, for which there is currently no effective treatment. Our previous studies have shown that *Lycium barbarum* (*L. barbarum*) polysaccharide (LBP) protects degenerated photoreceptors in rd1, a transgenic mouse model of retinitis pigmentosa. *L. barbarum* glycopeptide (LbGP) is an immunoreactive glycoprotein extracted from LBP. In this study, we investigated the potential protective effect of LbGP on a chemically induced photoreceptor-degenerative mouse model. Wild-type mice received the following: oral administration of LbGP as a protective pre-treatment on days 1–7; intraperitoneal administration of 40 mg/kg N-methyl-N-nitrosourea to induce photoreceptor injury on day 7; and continuation of orally administered LbGP on days 8–14. Treatment with LbGP increased photoreceptor survival and improved the structure of photoreceptors, retinal photoresponse, and visual behaviors of mice with photoreceptor degeneration. LbGP was also found to partially inhibit the activation of microglia in N-methyl-N-nitrosourea-injured retinas and significantly decreased the expression of two pro-inflammatory cytokines. In conclusion, LbGP effectively slowed the rate of photoreceptor degeneration in N-methyl-N-nitrosourea-injured mice, possibly through an anti-inflammatory mechanism, and has potential as a candidate drug for the clinical treatment of photoreceptor degeneration.
Key Words: anti-inflammation; inherited retinal diseases; *Lycium barbarum* glycopeptide; N-methyl-N-nitrosourea; opsin; photoreceptor; reactive gliosis; retinal degeneration; retinitis pigmentosa

Introduction

Photoreceptor degenerative diseases are a group of retinal diseases that include retinitis pigmentosa (RP), age-related macular degeneration, Stargardt's disease, and other inherited retina dystrophies. These diseases involve degeneration of the photoreceptors and loss of the ability to convert light into electrical signals, ultimately leading to blindness (Cai et al., 2019). RP is one of the most common forms of inherited retinal disease, causing degeneration and death of cone and rod cells (Hartong et al., 2006) and affecting approximately 1 in

4000 individuals worldwide (Verbakel et al., 2018). Age-related macular degeneration is another serious blinding condition, affecting about 8.7% of older people worldwide (Wong et al., 2014). The diverse genetic pathophysiology underlying these retinal degenerative diseases presents significant challenges in the development of effective treatments. The genetic basis of these diseases involves various mutations and gene abnormalities that lead to degeneration and dysfunction of photoreceptor cells in the retina (Dias et al., 2018; Leinonen et al., 2023). Several therapeutic approaches aimed at restoring or compensating for the loss of retinal function have been developed, such as stem cell therapy, gene therapy, retinal prostheses, and various drug therapies (Wang et al., 2019). However, the prospects of such treatments remain uncertain due to high costs, unpredictable adverse effects, and the technical difficulty of related surgeries. Therefore, the search for new treatment options for photoreceptor degeneration has become urgent.

Lycium barbarum (*L. barbarum*), commonly known as goji berry, is a popular traditional Chinese medicine known for its protective effects on the eyes (Neelam et al., 2021). *L. barbarum* polysaccharide (LBP), one of the major active ingredients of *L. barbarum*, has been extensively studied and has shown promising protective effects against various eye diseases, including glaucoma (Mi et al., 2012), retinal photodamage (Tang et al., 2018), RP (Wang et al., 2014; Liu et al., 2018) and diabetic retinopathy (Yao et al., 2018). In recent years, continuous improvements in the extraction process have led to the extraction of *L. barbarum* glycopeptide (LbGP) from LBP (Tian et al., 1995). LbGP is a glycoprotein with immunological activity, and the ability to reverse apoptotic resistance in aging T cells (Yuan et al., 2008), reduce inflammation and enhance autophagy in a kidney-protective manner (Zhou et al., 2022). It can also ameliorate aversive stimuli-induced depression by inhibiting microglial activation (Fu et al., 2021). However, whether LbGP can protect retinal neurons against retinal diseases is unclear.

In this study, we explored the protective effect of LbGP against mouse retinal injury induced by N-methyl-N-nitrosourea (MNU). MNU is a toxic alkylated substance that induces specific apoptosis of photoreceptor cells and is widely used in the chemically induced mouse model of photoreceptor degeneration (Tao et al., 2015).

Methods

Animals
Male C57BL/6J (C57) mice (specific pathogen-free grade; weight, ~21 g; age, 7 weeks) were purchased from Liaoning Changsheng Biotechnology Co., Ltd. (Benxi, Liaoning Province, China; License No. SCXK (Liao) 2020-0001). During the experimental period, all mice were kept in the Animal Breeding Center of Jinan University, which is equipped to provide standard laboratory conditions (humidity, 40–65%; room temperature, 18–23°C; dark/light cycle of 12/12 hours). Mice had free access to regular food and water. All animal experiments performed in this study adhered to the guidelines set forth by the Association for Research in Vision and Ophthalmology Statements for the Use of Animals in

Ophthalmic and Vision Research (Association for Research in Vision and Ophthalmology, 2021), and we made every effort to minimize the pain and suffering of the study animals. The Laboratory Animal Ethics Committee of Jinan University approved the experimental protocol on March 1, 2022 (approval No. IACUC-20220301-08).

Experimental design and drug application
The study animals were arbitrarily divided into three groups: untreated C57 mice that served as normal controls (Con, *n* = 46); MNU-injured mice (MNU, *n* = 47); and MNU-injured mice with LbGP treatment (LbGP, *n* = 47). Randomization of subjects to groups was not performed. LbGP (powder; purity ≥ 92.0%; Tianren Goji Biotechnology Co., Ltd., Zhongwei, Ningxia, China) was dissolved in phosphate-buffered saline (PBS) containing 0.1% dimethyl sulfoxide (0.1% PBS). Research has shown that LbGP is effective at doses of up to 100 mg/kg and is free of adverse effects (Zhou et al., 2022). Accordingly, in a preliminary experiment, we tested LbGP at doses of 5, 10, and 20 mg/kg body weight and found slight protection from photoreceptor degeneration, with more protective effects at higher doses. Based on the study conducted by Wu (2022), the protective effect of 50 mg/kg of LbGP was not particularly significant. Considering both the safety and effectiveness of the experiment, we have increased the dosage to 100 mg/kg. The mice were orally fed with LbGP daily for 2 weeks (days 1–14). On day 7, MNU (Shanghai Macklin Biochemical Technology Co., Ltd, Shanghai, China) solution (40 mg/kg in normal saline) was injected intraperitoneally to induce specific photoreceptor degeneration (Yuge et al., 1996; Emoto et al., 2013; Hayakawa et al., 2020). On day 15, visual behavior was examined. On day 16, electroretinogram (ERG) tests were administered, the animals were sacrificed, and retinas were collected. The detailed protocol for the experimental procedures is illustrated in **Figure 1**.
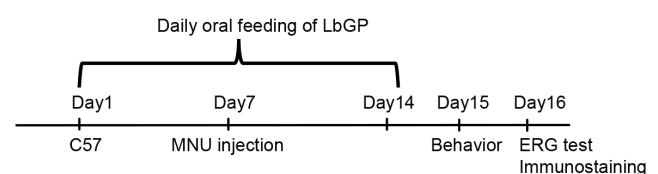
Figure 1 | **Experimental design.**
Adult C57 mice were orally fed with LbGP daily for 14 days. On day 7, 40 mg/kg MNU was intraperitoneally injected to induce retinal photoreceptor cell degeneration. On day 15, visual behaviors were examined, and on day 16, an electroretinogram (ERG) was recorded, the mice were sacrificed, and retinas were collected for immunostaining. C57: C57BL/6J mice; ERG: electroretinogram; LbGP: *Lycium barbarum* glycopeptide; MNU: N-methyl-N-nitrosourea.

Black-white transition test
On day 15, following 2 weeks of LbGP treatment, we administered a black-white transition test to evaluate the ability of the mice to discriminate differences in luminance, as previously described (Zhang et al., 2022a). The black and white conversion system, manufactured by Metronet Technology Co. (Beijing, China), consists of a black box and a white box, each with dimensions of 16 cm × 16 cm × 25 cm. The mice move between the two boxes through a small door

under an opaque baffle. Mice with normal vision tended to stay in darkness, and thus spent longer periods in the black box. Infrared cameras were mounted under the lid above each box to capture the movement of the mice inside. We used EthoVision XT 8.0 analysis software (Doldus, Wageningen, Netherlands) to analyze the moving trajectories of mice in both boxes and to calculate the time spent in both boxes over a 5-minute test period. The amount of time spent in the black box was used as an indicator of the luminance discrimination ability.

Optomotor test

After 2 hours of dark adaptation, the experimental mice underwent visual acuity testing using an optomotor system programmed by Matlab 8.0 software (MathWorks, Natick, MA, USA) (Liu et al., 2021). The mice were placed on a cylindrical test elevation surrounded by four monitors displaying rotating sine gratings of different spatial frequencies programmed by Matlab 8.0. The gratings had a 100% contrast and moving speed of 12 cycles/s, with increasing spatial frequencies ranging from 0.1 to 0.6 cycles/degree. The movement of each animal was videotaped, and any head movement tracking the rotating gratings was manually recorded as an optomotor reflex by independent observers. The maximal spatial frequency of the grating that triggered the optomotor reflex was considered to represent the visual acuity of the animal.

ERG

To observe the effects of LbGP on retinal function, mice were subjected to ERG tests on day 16, after an overnight dark adaptation, using the RETI-scan system (Roland Consult, Brandenburg, Germany) and following a protocol we described previously (Zhang et al., 2017). Briefly, the animals were anesthetized by intraperitoneal injection of a 1.25% tribromoethanol solution (0.02 mL/g; Merck KGaA, Darmstadt, Germany) and positioned on a 37°C heating platform. Recording electrodes were placed on the corneal surface, and ground and reference needle electrodes were inserted in the tail and skin near the eye, respectively. The mice were stimulated with full-field green flashes under dark adaptation (scotopic vision), with intensities of 0.01, 0.1, and 3.0 cd/m^2. Next, they were light adapted to a green background of 20 cd/m^2 for 5 minutes, and the photopic responses to a green flash with an intensity of 10.0 cd/m^2 were recorded. ERG data were collected and analyzed by RETIport software (Roland Consult, Brandenburg, Germany). The recorded signal presented as a negative peak (a-wave, representing the group responses of photoreceptors) after light onset, followed by a positive peak (b-wave, representing group responses of bipolar cells). The a- and b-wave amplitudes were measured by RETI software. The optimal response for two eyes was chosen as the data for each mouse. Mice were classified as responsive to light on the basis of a measurable light-induced ERG response.

Tissue processing

After completion of the ERG test, the still-anesthetized mice were immediately euthanized by cervical dislocation. The eyes were removed, enucleated, and immersed in 4% paraformaldehyde for 30 minutes at room temperature,

then washed three times with 0.1% PBS buffer solution for 5 minutes each time and dehydrated overnight in 24-well plates containing 30% sucrose solution. The dehydrated tissues were placed in boxes containing optimum cutting temperature compounds (Tissue Tek, Torrance, CA, USA) and immediately transferred to a freezer at –40°C. Retinas were cryosectioned longitudinally through the optic disk using a microtome (Leica Microsystems, Wetzlar, Germany) at 14 μm thickness. The retinal sections were then mounted onto glass slides for subsequent processing.

Immunofluorescent staining

For staining, retinal sections were treated as follows: three washes with 0.3% PBS containing 0.3% Triton X-100 (PBST) for 5 minutes each time; incubation in blocking solution (3% bovine serum albumin and 5% normal donkey serum in 0.3% PBST) for 2 hours; incubation with primary antibodies overnight at 4°C: cleaning followed by incubation with the secondary antibody for 2 hours at room temperature; sealing and storage in a 4°C refrigerator before imaging. To stain the cell nuclei, sections were subjected to a 5-minute treatment with 4′,6-diamidino-2-phenylindole before being mounted. Detailed information on primary antibodies, secondary antibodies, and fluorescent dyes is listed in **Table 1**.

Image collection and processing

Immunofluorescence-stained tissues were imaged using a confocal microscope (Zeiss LSM700, Oberkochen, Germany) or a fluorescence microscope (Zeiss Axio Imager A2). To evaluate photoreceptor survival, the thickness and number of cell layers in the outer nuclear layer (ONL), where the photoreceptor somas are located, were measured and counted, respectively. To count the cell layers, a line vertical to the retinal layers was drawn and the 4′,6-diamidino-2-phenylindole-stained nuclei located on the line were counted. Due to the unevenness of the retinal ONL during MNU-induced degeneration, the ONL thickness was measured at 400, 800, 1200, and 1600 μm away from the central point of the optic nerve on both sides. To assess photoreceptor structure, the outer segment (OS) length of the cones (stained by opsin) and the OS thickness of the rods (stained by rhodopsin) were measured at a location 800 μm away from the optic nerve center. Also in this region, we quantified the fluorescence intensity of glial fibrillary acidic protein (GFAP) and its accumulated fluorescent area as indicators of the status of Müller glial cells. Different groups of retinal sections were treated with the same immunostaining processing and imaging parameters. To access the activation status of microglia, we counted the number of cells positive for ionized calcium-binding adaptor molecule-1 (Iba-1) within clusters of differentiation 68 (CD68)-positive cells in three regions of the retina: the center (400 μm), middle (800 μm), and periphery (1200 μm) (image size, 624.7 μm × 501.22 μm). Image-Pro Plus software (Media Cybernetics, Rockville, MD, USA) was used for all measurements and analysis of immunofluorescence. Measurements from three retinal sections were averaged to obtain one value for each mouse. These values were further averaged to obtain an overall average value for the entire group.

Table 1 | Antibody-specific information

Antibody	Species	Concentration	Company	Cat#	RRID
Rhodopsin	Mouse	1:1000	Millipore, Burlington, MA, USA	MAB5356	AB_2178961
Opsin	Rabbit	1:1000	Millipore	AB5405	AB_177456
GFAP	Rat	1:1000	Thermo Fisher Scientific, Waltham, MA, USA	13-0300	AB_2532994
Iba-1	Rabbit	1:1000	FUJIFILM WAKO SHIBAYAGI, Shibayagi, Japan	019-19741	AB_839504
CD68	Mouse	1:1000	Abcam, Cambridge, UK	ab31630	AB_1141557
Mouse IgG (H+L) Highly Cross-Adsorbed Secondary Antibody, Alexa Fluor™ 488	Donkey	1:1000	Invitrogen, Waltham, MA, USA	A-21202	AB_141607
Rabbit IgG (H+L) Highly Cross-Adsorbed Secondary Antibody, Alexa Fluor™ 488	Donkey	1:1000	Invitrogen	A-21206	AB_2535792
Rat IgG (H+L) Highly Cross-Adsorbed Secondary Antibody, Alexa Fluor™ 488	Donkey	1:1000	Invitrogen	A-21208	AB_2535794
Mouse IgG (H+L) Highly Cross-Adsorbed Secondary Antibody, Alexa Fluor™ 647	Donkey	1:1000	Invitrogen	A-31571	AB_162542
Rabbit IgG (H+L) Highly Cross-Adsorbed Secondary Antibody,Alexa Fluor™ 647	Donkey	1:1000	Invitrogen	A-31573	AB_2536183
DAPI Fluoromount G	Donkey	1:1000	Electron Microscopy Sciences, Hatfield, PA, USA	17984-24	

CD68: Cluster of differentiation 68; DAPI: 4′,6-diamidino-2-phenylindole; GFAP: glial fibrillary acidic protein; Iba-1: ionized calcium-binding adapter molecule-1; IgG (H+L): immunoglobulin G (heavy and light chains).

Real-time quantitative polymerase chain reaction

We used real-time quantitative polymerase chain reaction (RT-qPCR) to detect changes in the expression of inflammation-related genes (Sun et al., 2017). Retinas were dissected, placed in TRIzol™ Reagent (Cat# 15596026; Invitrogen, Thermo Fisher Scientific, Shanghai, China), and the RNA was extracted in accordance with the manufacturer's protocol. The purity and concentration of RNA were measured using a NanoDrop 2000C ultra-micro spectrophotometer (Thermo Fisher Scientific [Shanghai] Co., Ltd, Shanghai, China). A PrimeScript™ RT kit with gDNA Eraser (Perfect Real Time; Takara Biomedical Technology [Beijing] Co., Ltd., Beijing, China) was used to obtain complementary DNA templates (85°C for 5 seconds), which were then diluted 5-fold with RNase/Dnase-free water. We designed the primers for qPCR in the primer library (https://www.ncbi.nlm.nih.gov/tools/primer-blast/) and synthesized them at Sangon Biotech (Shanghai, China). **Table 2** lists the primers used in this experiment. We performed real-time RT-qPCR using TB Green® Premix Ex Taq™ II (Tli RNaseH Plus) (Takara Biomedical Technology [Beijing] Co., Ltd.) and a LightCycler 480 system (F. Hoffmann-La Roche Ltd., Basel, Switzerland), in accordance with the operating instructions. The glyceraldehyde-3-phosphate-dehydrogenase gene (Gapdh) was used as an internal control. PCR conditions were as follows: pre-denaturation for one cycle of 95°C for 30 seconds; 40 cycles of 95°C for 5 seconds and 60°C for 30 seconds; one cycle of 95°C for 5 seconds, 60°C for 60 seconds, and 95°C for 15 seconds; and a final cooling step of 50°C for 30 seconds. We used the comparative Ct method to calculate fold changes in expression (Livak and Schmittgen, 2001).

Statistical analysis

Although we did not use statistical methods to determine the sample size, our sample size was similar to that reported in a previous publication (Xiang et al., 2018). Data are presented as the mean ± standard error of the mean (SEM). Data were analyzed using a one-way analysis of variance followed by Tukey's *post hoc* test performed by GraphPad Prism version 9.0.0 for Windows (GraphPad Software, Boston, MA, USA; www.graphpad.com). P values < 0.05 were considered to indicate statistical significance. The total number of mice tested in each group is represented by n values.

Table 2 | Real-time polymerase chain reaction primers

Target gene	Sequence (5' to 3')
GAPDH	Sense: CAT GGC CTT CCG TGT TCC TA
	Anti-sense: CCT GCT TCA CCA CCT TCT TGA T
NF-κB	Sense: ACA GAG GCC ATT GAA GTG A
	Anti-sense: CGT GGA GGA AGA CGA GAG
HIF-1	Sense: ACC TTC ATC GGA AAC TCC AAA G
	Anti-sense: ACC TTC ATC GGA AAC TCC AAA G
IL-1β	Sense: ACC TTC ATC GGA AAC TCC AAA G
	Anti-sense: ACC TTC ATC GGA AAC TCC AAA G
iNOS	Sense: AAT GGC AAC ATC AGG TCG GCC ATC ACT
	Anti-sense: GCT GTG TGT CAC AGA AGT CTC GAA CTC
CD40	Sense: ACC TTC ATC GGA AAC TCC AAA G
	Anti-sense: ACC TTC ATC GGA AAC TCC AAA G
IL-6	Sense: TAG TCC TTC CTA CCC CAA TTT CC
	Anti-sense: TAG TCC TTC CTA CCC CAA TTT CC

CD40: Tumor necrosis factor receptor; GAPDH: glyceraldehyde-3-phosphate dehydrogenase; HIF-1: hypoxia inducible factor-1; IL-1β: interleukin-1β; IL-6: interleukin-6; iNOS: inducible nitric oxide synthase; NF-κB: nuclear factor kappa-B.

Results

LbGP improves visual behaviors of MNU-injured mice

To explore the impact of LbGP on the visual behavior of photoreceptor-degenerative mice, we first examined their ability to visually discriminate differences in luminance using a black-white transition box. Because mice tend to remain in darkness to avoid light, their ability to detect luminance can be assessed from the amount of time they spend in the black box. Con group mice stayed longer in the black box than in the white box, whereas MNU group mice spent essentially equal amounts of time in both boxes. LbGP treatment restored the time spent in darkness to that of the Con group (example of movement trace shown in **Figure 2A**). Statistically, MNU-injured mice spent 27.7% less time in the black box than Con mice, indicating that MNU group mice had an impaired ability to detect light. In the LbGP-treated group of photoreceptor-degenerative mice, the residence time in the black box was extended by 14.0% compared with the MNU group (n = 10, P < 0.05; **Figure 2B**).

Next, we tested visual acuity using the optomotor response test (**Figure 2C**), which measures the ability of mice to distinguish fine spatial frequency objects by monitoring head

tracking in the direction of the rotating gratings. Higher spatial frequencies (corresponding to thinner gratings) that trigger an optokinetic response indicate higher visual acuity in the animals (Milla-Navarro et al., 2022). The results showed a 71.1% decrease in visual acuity in MNU-injured mice compared with the control, and LbGP treatment increased it 2-fold ($n = 6$, $P < 0.05$, compared to the MNU group; **Figure 2D**). Therefore, treatment with LbGP before and after MNU-induced retinal injury greatly improved visual behaviors in mice.
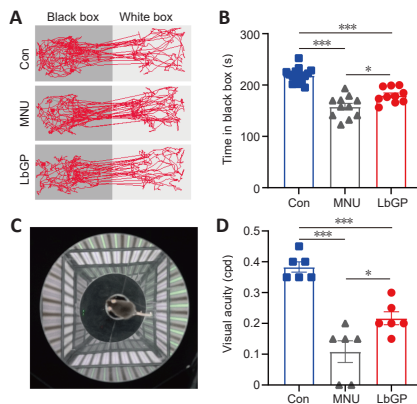

Figure 2 | LbGP improves visual behaviors in MNU-injured mice.
(A) Motion trajectories of the mice in black-white transition tests of each group. (B) Duration of time spent in the black box for each group: Con group, $n = 16$; MNU group, $n = 11$; LbGP group, $n = 10$. (C) Illustration of the optomotor system. (D) Visual acuity (in cycles per degree, cpd) for each group ($n = 6$/group). LbGP treatment increased the time that photoreceptor-degenerative mice spent in the black box, as well as their visual acuity. Data are expressed as mean ± standard error of the mean; *$P < 0.05$, ***$P < 0.001$ (one-way analysis of variance followed by Tukey's *post hoc* test). Con: C57BL/6J mice; LbGP: N-methyl-N-nitrosourea-injured mice with *Lycium barbarum* glycopeptide treatment; MNU: N-methyl-N-nitrosourea-injured mice without treatment.

LbGP improves retinal light response in MNU-injured mice

Next, we examined the possible effect of LbGP on the retinal light response using ERG recording. The a- and b-waves in ERG traces represent the group light responses in photoreceptor and bipolar cells, respectively. Better retinal responses correlate with larger amplitudes of a- and b-waves and shorter latency periods of a- and b-wave peaks (Creel, 2019). Neurons with good flash response are present in the normal mouse retina, in both dark- and light-adapted conditions. In our MNU-injured mice, photoreceptor degeneration led to greatly reduced or even abrogated light responses that were partially restored by LbGP treatment (**Figure 3A**). While 100% of the Con group mice were clearly responsive to light, only 62% of MNU group mice and 80% of LbGP group mice exhibited light responsiveness (**Figure 3B**). Analysis of the amplitudes of scotopic a- and b-waves showed that LbGP treatment led to significant improvements compared to the untreated MNU group for most flash intensities, although the amplitudes were still lower than those in the Con group (Scotopic 3.0 a- and b-waves: $P = 0.001$ and $P = 0.0048$, respectively; **Figure 3C**). At the light intensity of Scotopic 3.0, LbGP also tended to reduce the a- and b-wave latencies compared with MNU group mice, but the differences were not significant (a- and b-waves: $P = 0.6597$ and $P = 0.9463$, respectively; **Figure 3D**). For ERG responses under light adaptation, LbGP treatment provided only minimal improvement in the retinal light response (**Additional Figure 1**).
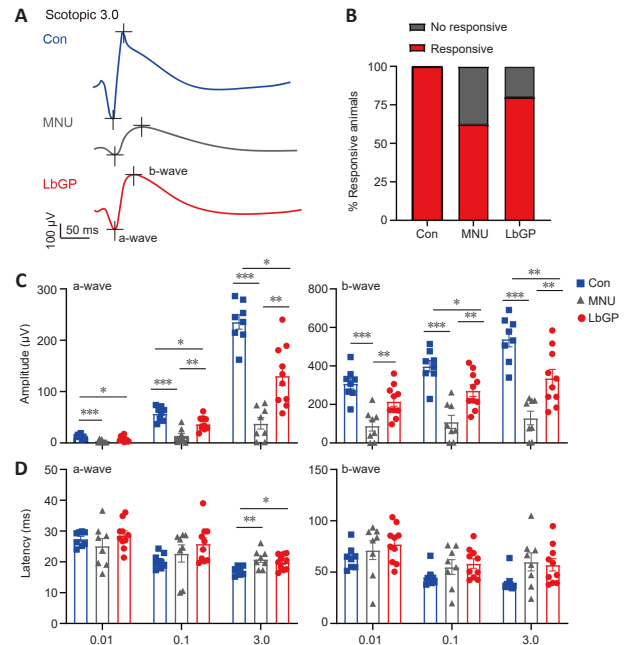

Figure 3 | LbGP enhances the retinal light responses of photoreceptor-degenerative mice.
(A) Representative electroretinogram traces of each group to flashes at Scotopic 3.0 cd·s/m². (B) Proportions of mice with (Con, $n = 8$; MNU, $n = 8$; LbGP, $n = 10$) and without (Con, $n = 0$; MNU, $n = 3$; LbGP, $n = 2$) responsiveness to light in each group. (C) Peak amplitudes of the a- and b-waves under scotopic conditions for each flash intensity (Con, $n = 8$; MNU, $n = 8$; LbGP, $n = 10$). (D) Latency of the a- and b-waves, showing increased retinal light responses under LbGP treatment (Con, $n = 8$; MNU, $n = 8$; LbGP, $n = 10$). Data are expressed as mean ± standard error of the mean; *$P < 0.05$, **$P < 0.01$, ***$P < 0.001$ (one-way analysis of variance followed by Tukey's *post hoc* test). Con: C57BL/6J mice; LbGP: N-methyl-N-nitrosourea-injured mice with *Lycium barbarum* glycopeptide treatment; MNU: N-methyl-N-nitrosourea-injured mice without treatment.

LbGP preserves retinal structures in MNU-injured mice

Responses assessed by ERG were improved in LbGP-treated mice, suggesting that LbGP slowed the MNU-induced cellular degeneration of photoreceptors. Therefore, we examined the survival and structures of photoreceptors in these mice by immunostaining. Because the effects of MNU may vary from the center to the periphery of the retina (Tao et al., 2015), we examined the morphological changes induced by MNU at different regions of the retina. **Figure 4A** and **B** shows typical images of a retinal section from the intermediate region in each group. Compared with the Con group, the ONL (where the photoreceptor soma are located) was much thinner, with fewer cell layers, in the MNU group, but showed improvements in terms of thickness and number of cell layers in the LbGP group. At 800 μm from either side of the optic nerve center, the number of cell layers and the thickness of the ONL were significantly reduced in the MNU group compared to those in the Con group ($P = 0.0047$) and were improved in the LbGP group ($P = 0.0038$; **Figure 4C** and **D**). The 800-μm location showed the greatest effects of LbGP: ONL thickness, which was reduced by 63.9% in the MNU group compared to that in the Con group, was increased by 72.1% in the LbGP group ($n = 8$, $P < 0.01$ compared to the MNU group; **Figure 4D**), while the number of cell layers in the ONL increased by 65.5% in the LbGP group ($n = 8$, $P < 0.01$ compared to the MNU group; **Figure 4C**).

We conducted further examinations of the cone and rod structures by immunostaining the OSs using antibodies against

opsin and rhodopsin, respectively (Carroll et al., 2012). While the OS of the cones in the Con group presented as long strips, those in the MNU group were barely stained, with only a few dots; however, LbGP restored the morphology of long strips (**Figure 4A**). Similarly, the OS of rods showed a clear, thick layer of immunostaining in the Con group that was greatly reduced in the MNU group and restored in the LbGP group (**Figure 4B**). In the intermediate region of the retina (800 μm), compared with the Con group, measurements of OS thickness of cones and rods were decreased by 73.5% and 73.7%, respectively, in the MNU group ($n = 8$, $P < 0.01$). By contrast, compared with the MNU group, the LbGP group showed increases in cone and rod OS thickness of 143.6% and 86.03%, respectively ($n = 8$, $P < 0.01$; **Figure 4E** and **F**).

effect of LbGP on degeneration of the retina. Reactive gliosis, a hallmark of retinal inflammation, is characterized by the activation of microglia and Müller cells (Bringmann et al., 2009). Because LbGP has an anti-inflammatory effect (Huang et al., 2022), we examined whether LbGP inhibited reactive gliosis. The activation of microglia was examined by immunostaining for the activated microglial markers Iba-1 (markers of microglia) (Kotliarova and Sidorova, 2021) and CD68 (markers of active microglia) (Slepko and Levi, 1996). In the normal retinas of Con group mice, there was negligible expression of Iba-1 and CD68, indicating minimal microglial activation and phagocytic activity. MNU group mice showed significantly increased retinal expression of CD68 and Iba-1, indicating increased microglial activation, and a considerable number of microglia with reactive morphology characterized by an amoeboid shape. LbGP treatment reduced the expression of both Iba-1 and CD68 (**Figure 5A–C**). In all retinal regions from the center to the periphery, compared to the MNU group, the LbGP group showed significantly reduced numbers of Iba-1-positive cells ($n = 3$, $P < 0.05$; **Figure 5D**) and a tendency for reduced CD68-positive cells ($n = 3$, $P > 0.05$, compared to MNU group, **Figure 5E**). Therefore, we concluded that LbGP inhibited the reactivation of microglia in the MNU-injured retina.
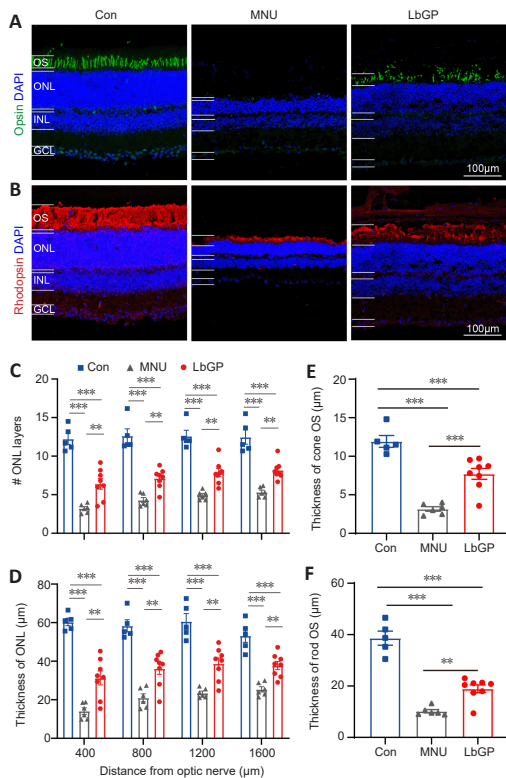

Figure 4 | LbGP improves photoreceptor structure and survival in the MNU-injured retina.
(A, B) Representative images of retinal sections from the intermediate region of each group. Opsin (Alexa Fluor™ 488, green; A) and rhodopsin (Alexa Fluor™ 647, red; B) immunostaining was used to label the outer segment (OS) of the cones and rods, respectively. Areas of retinal opsin and rhodopsin staining formed elongated or columnar shapes in the normal control (Con) group, dots or clumps in the MNU group, and long stripe shapes in the LbGP group retina. The nuclei were stained with 4,6-diamino-2-phenyl indole (DAPI; blue). Scale bars: 100 μm. (C, D) Quantification of the cell layers (C) and thickness (D) of the outer nuclear layer (ONL). In each group, retinal sections were evaluated from the center to the peripheral regions. (E, F) Thickness of the OS of cones (E) and rods (F) in each group. The ONL and OS measurements of the cones and rods were significantly thinner in the retinas of the MNU group than those in the Con group. Treatment with LbGP significantly increased these parameters. Data expressed as mean ± standard error of the mean (Con, $n = 5$; MNU, $n = 6$; LbGP, $n = 8$); **$P < 0.01$, ***$P < 0.001$ (one-way analysis of variance followed by Tukey's *post hoc* test). Con: C57BL/6J mice; DAPI: 4′,6-diamidino-2-phenylindole; GCL: ganglion cell layer; INL: inner nuclei layer; LbGP: N-methyl-N-nitrosourea-injured mice with *Lycium barbarum* glycopeptide treatment; MNU: N-methyl-N-nitrosourea-injured mice without treatment; ONL: outer nuclei layer.

LbGP partially inhibits microglial activation in the MNU-injured retina

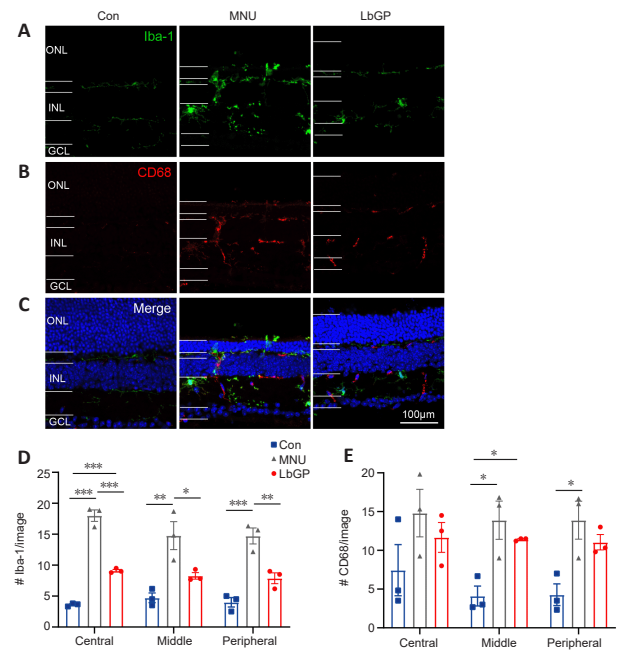We also investigated possible mechanisms for the protective

Figure 5 | LbGP partially inhibits microglial activation in the MNU-injured retina.
(A–C) Representative images of retinal slices stained with Iba-1 (green, Alexa Fluor-488; top panels, marker for microglia), CD68 (red, Alexa Fluor-647; middle panels, a marker of activated macrophages and microglia), and DAPI (blue; bottom panels). Microglia in the retinas of the Con group were essentially quiescent, whereas microglia in the retinas of the MNU group were activated, with enlarged cytosolic bodies and increased branching. This activation was attenuated in the retinas of the LbGP group. Scale bars: 100 μm. (D, E) Numbers of Iba-1-positive (D) and CD68-positive cells (E) per image (size, 625 μm × 501 μm) at the central, middle, and peripheral locations of the retina. LbGP decreased the number of Iba-1-positive cells. Data are expressed as mean ± standard error of the mean ($n = 3$/group); *$P < 0.05$, **$P < 0.01$, ***$P < 0.001$ (one-way analysis of variance followed by Tukey's *post hoc* test). Con: C57BL/6J mice; DAPI: 4′,6-diamidino-2-phenylindole; GCL: ganglion cell layer; INL: inner nuclei layer; LbGP: N-methyl-N-nitrosourea-injured mice with *Lycium barbarum* glycopeptide treatment; MNU: N-methyl-N-nitrosourea-injured mice without treatment; ONL: outer nuclei layer.

Next, we observed the status of Müller glial cells, which play a crucial role in maintaining retinal homeostasis (Bringmann et al., 2009), in each group. The activation of Müller cells is indicated by increased GFAP expression in the cell processes (Bringmann et al., 2006). In Con group retinas, Müller glial cells did not exhibit any signs of activation, and GFAP expression was mainly restricted to the astrocytes in the ganglion cell layer and was accompanied by short dendritic extensions. In MNU group retinas, there was a marked increase in GFAP expression in the processes of Müller glial cells. These processes exhibited strong GFAP immunoreactivity and extended from the ganglion cell layer to the ONL, indicating a pronounced activation of Müller glial cells. The LbGP treatment group showed only a slight decrease in retinal GFAP expression ($n = 4$, $P > 0.05$ compared to the MNU group; **Figure 6**). We concluded that, in the MNU-injured retina, LbGP partially inhibited microglial activation but did not affect Müller cells.
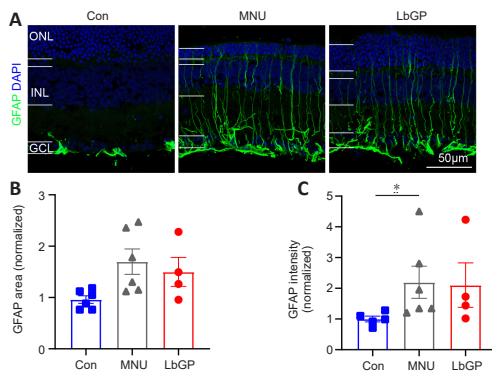

Figure 6 | **LbGP hardly inhibits Müller glial cell activation in the MNU-injured retina.**
(A) Representative images of retinal sections stained with GFAP (Alexa Fluor-488, green) and DAPI (blue) for each group. In both the untreated and LbGP-treated MNU-injured mice, GFAP expression in Müller glial cells was present throughout the retina. Scale bars: 50 μm. (B, C) Fluorescence area (B) and intensity (C) of GFAP-positive regions (normalized to the control) of each group. Data expressed as mean ± standard error of the mean (Con, $n = 5$; MNU, $n = 6$; LbGP, $n = 4$); *$P < 0.05$ (one-way analysis of variance followed by Tukey's *post hoc* test). DAPI: 4′,6-Diamidino-2-phenylindole; GCL: ganglion cell layer; GFAP: glial fibrillary acidic protein; INL: inner nuclei layer; LbGP: N-methyl-N-nitrosourea-injured mice with *Lycium barbarum* glycopeptide treatment; MNU: N-methyl-N-nitrosourea-injured mice without treatment; ONL: outer nuclei layer.

LbGP inhibits pro-inflammatory cytokine expression in the MNU-injured retina

Because our immunostaining results demonstrated partial inhibition of retinal inflammation by LbGP, we used RT-qPCR to further examine its role in the expression of the following pro-inflammatory factors: nuclear factor kappa-B (NF-κB), interleukin (IL)-1β, IL-6, hypoxia-inducible factor-1 (HIF-1), inducible nitric oxide synthase (iNOS), and CD40. Overall, compared with the Con group, we observed elevated mRNA expression of all six pro-inflammatory cytokines in the MNU group retinas (**Figure 7A–F**). These changes in the MNU group were reversed in the LbGP-treated group, which showed reductions in the mRNA levels of all six pro-inflammatory cytokines, with significant differences in NF-κB ($n = 4$, $P < 0.01$; **Figure 7A**) and HIF-1 ($n = 4$, $P < 0.05$; **Figure 7D**).

Discussion

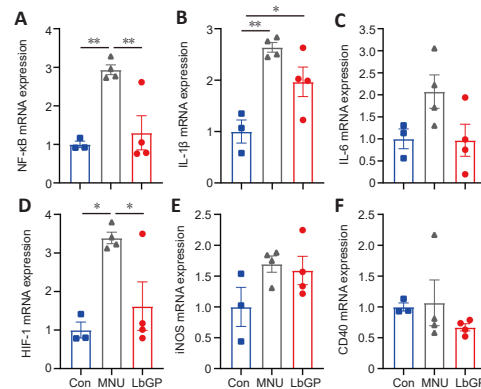Our experimental results demonstrated that LbGP improved

Figure 7 | **LbGP decreases the mRNA expression of pro-inflammatory cytokines in the MNU-injured retina.**
(A–F) mRNA expression of the indicated pro-inflammatory cytokines in each group. LbGP significantly reduced the MNU-induced upregulation of nuclear factor (NF)-κB and hypoxia-inducible factor (HIF)-1, but not the other cytokines, in the retinas of photoreceptor-degenerative mice. Data expressed as mean ± standard error of the mean (Con, $n = 3$; MNU, $n = 4$; LbGP, $n = 4$); *$P < 0.05$, **$P < 0.01$ (one-way analysis of variance followed by Tukey's *post hoc* test). CD40: Tumor necrosis factor receptor superfamily 5; Con: C57BL/6J mice; HIF-1: hypoxia-inducible factor-1; iNOS: inducible nitric oxide synthase; IL-1β: interleukin-1 beta; IL-6: interleukin-6; LbGP: N-methyl-N-nitrosourea-injured mice with *Lycium barbarum* glycopeptide treatment; MNU: N-methyl-N-nitrosourea-injured mice without treatment; NF-κB: nuclear factor kappa-B.

the morphological structures and survival of photoreceptors in MNU-induced photoreceptor-degenerative mice. LbGP also improved retinal photo-response and visual behavior. Taken together, our results indicated that LbGP effectively protects photoreceptor structure and retinal function in these mice.

MNU is an alkylating agent that specifically targets and damages photoreceptor cells in the retina, leading to their degeneration and loss of function (Tsubura et al., 2011; Xiong et al., 2016). Therefore, animals injured by MNU have been commonly applied as good models for human RP and other photoreceptor-degenerative diseases (Yoshizawa et al., 1999; Ma et al., 2006; Deng et al., 2021). Other animal models of photoreceptor degeneration include rd10 and rd1 mice, which carry mutations in Pde6β that lead to defective phototransduction and subsequent death of rod cells (Chang et al., 2002). Because variations in PDE6β are known to cause clinical RP in patients, these mouse models are commonly used to study rod-specific degeneration, providing deep insight into the pathogenesis of RP. However, while both rd10 and rd1 mice lose most of their rods before reaching adulthood, clinical RP patients lose vision in adulthood. By contrast, in MNU models, photoreceptor degeneration can be induced in adult or even aged mice. Furthermore, because the extent of MNU-induced injury is dose-dependent, different stages of RP pathogenesis can be simulated by varying the dose, which holds clinical significance (Yang et al., 2004). Hence, the MNU injury model offers valuable insights into the potential dose-dependent effects of LbGP and its therapeutic implications for different stages of RP.

We found that the protective effect of LbGP on degenerated retinas was comparable to that of LBP, from which LbGP is extracted. A few studies have demonstrated that LBP administered by oral gavage or intraperitoneal injection can protect degenerated photoreceptors in various rodent models of RP, including transgenic mice, such as rd10 and

rd1 (Wang et al., 2014; Liu et al., 2018), and MNU-injured rats (Zhu et al., 2016). The dose of LBP ranged from 10 mg/kg to 400 mg/kg, with improved survival of photoreceptors reaching 50–80% of that in normal mice (Zhu et al., 2016; Liu et al., 2018). In our study, 100 mg/kg LbGP restored the rate of photoreceptor survival to over 60% of that in normal mice, which is comparable to that with LBP treatment. Notably, the extent of the protective effect of LbGP and LBP is dose dependent and is affected by the treatment timing (pre-treatment *vs.* treatment at an early or late stage of degeneration), administration method (oral feeding *vs.* intraperitoneal injection), and degeneration model (rats *vs.* mice, transgenic *vs.* chemical-induced injury). Therefore, LbGP may or may not be more advantageous than LBP. However, LbGP is an active small molecule peptide extracted from LBP; thus, it may be more easily absorbed by the human body. Furthermore, in our study, we administered LbGP by oral feeding, which is more convenient and clinically appropriate than intraperitoneal injection. Also, we chose a lower dose of MNU than the 60 mg/kg used by Zhu et al. (2016), which led to a slower degeneration of photoreceptors than a high dose. This is in line with the clinical reality: most patients do not wait until they lose their vision completely before seeking treatment but rather seek screening and treatment at an early stage of vision loss. Therefore, we chose the low dose of MNU for the retinal injury, aiming to provide timely intervention at an early stage of the disease and achieve the goal of saving the subject's vision. With a comparable protective effect and better absorbency than LBP, LbGP has good prospects for clinical application.

LbGP may exert its protective effect through anti-inflammation. In various RP models (including MNU-induced injury and transgenic mice), Müller cell proliferation and microglial activation were reported (Chen et al., 2014; Moon et al., 2017). Activation of both microglia and Müller cells can produce pro-inflammatory effects that act on photoreceptor cells, thus accelerating their death (Massengill et al., 2018; Silverman and Wong, 2018). Indeed, increased expression of pro-inflammatory cytokines was reported in the transgenic RP mouse model (Liu et al., 2021). In our current research, LbGP reduced microglial activation in the MNU-injured retina, and also inhibited the increased mRNA expression of pro-inflammatory cytokines, including HIF-1 and NF-κB, demonstrating its anti-inflammatory ability. Similar anti-inflammatory effects of *L. barbarum* extracts have been also reported in studies of retinal diseases, including diabetic retinopathy (Song et al., 2011) and age-related macular degeneration (Zheng et al., 2023). It is important to note that LbGP did not inhibit Müller cell gliosis or decrease the expression of other pro-inflammatory cytokines (such as iNOS, IL-1β, CD40, and IL-6), which may have contributed to the incomplete recovery of photoreceptor-degenerative mice in the LbGP group. Why the effects of LbGP were different in microglial cells and Müller cells is unclear. In our previous studies in rd10 mice, other protective agents, such as methyl-3,4-dihydroxybenzoate (Zhang et al., 2017), luteolin (Liu et al., 2021), and mesenchymal stem cell-derived extracellular vesicles (Zhang et al., 2022b) showed inhibition of both microglial and Müller cells, while LBP inhibited microglial

activation (Wang et al., 2014). However, the effects of LBP on Müller cells are rarely reported (Manthey et al., 2017). One *in vitro* study using a spinal cord injury model demonstrated that LBP does not directly affect astrocytes, which are phenotypically similar to Müller cells and astrocytes in the retina (Zhang et al., 2013). This is consistent with our current findings. Further study may be necessary to elucidate the reasons for the differential effects of LbGP on various types of glial cells and the varied expression of pro-inflammatory cytokines.

The current research has several limitations to consider. First, our study focused primarily on the anti-inflammatory effect of LbGP and did not investigate other possible protective mechanisms. Second, we only examined the effect of LbGP on MNU-induced photoreceptor degeneration for 14 days; thus, its potentially protective effect in the long term is unknown. Third, we pre-treated the mice with LbGP prior to MNU-induced injury to strengthen its protective effect; however, clinical treatment can only be applied after the diagnosis of the disease. It will be important to test whether the application of LbGP after disease onset also delays photoreceptor degeneration. A combination of LbGP with other bioactive components may also be considered to improve the protective effect. Fourth, additional experiment groups may add more information to this study, like LbGP treatment without MNU induction, and LbGP treatment before MNU induction only and post-induction only. Finally, the fifth limitation in this study was that only male mice were used; female mice should have been added to the experimental group.

In conclusion, our study demonstrated neuroprotective effects of LbGP in MNU-induced RP model mice, delaying the degeneration of photoreceptors and preserving retinal structure and function. Therefore, LbGP holds promise as a candidate for the clinical treatment of retinal degenerative diseases.

Additional file:
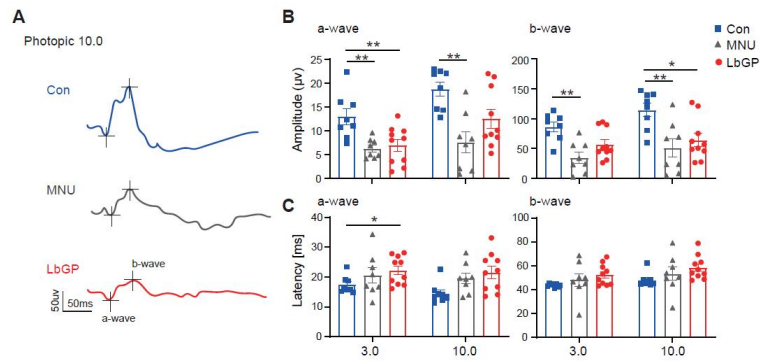*Additional Figure 1: The retinal light responses of photoreceptor degenerated mice.*

References

Association for Research in Vision and Ophthalmology (2021) ARVO Statement for the Use of Animals in Ophthalmic and Vision Research.

Bringmann A, Pannicke T, Grosche J, Francke M, Wiedemann P, Skatchkov SN, Osborne NN, Reichenbach A (2006) Müller cells in the healthy and diseased retina. Prog Retin Eye Res 25:397-424.

Bringmann A, Iandiev I, Pannicke T, Wurm A, Hollborn M, Wiedemann P, Osborne NN, Reichenbach A (2009) Cellular signaling and factors involved in Muller cell gliosis: neuroprotective and detrimental effects. Prog Retin Eye Res 28:423-451.

Cai Y, Cheng T, Yao Y, Li X, Ma Y, Li L, Zhao H, Bao J, Zhang M, Qiu Z, Xue T (2019) In vivo genome editing rescues photoreceptor degeneration via a Cas9/RecA-mediated homology-directed repair pathway. Sci Adv 5:eaav3335.

Carroll J, Dubra A, Gardner JC, Mizrahi-Meissonnier L, Cooper RF, Dubis AM, Nordgren R, Genead M, Connor TB, Jr., Stepien KE, Sharon D, Hunt DM, Banin E, Hardcastle AJ, Moore AT, Williams DR, Fishman G, Neitz J, Neitz M, Michaelides M (2012) The effect of cone opsin mutations on retinal structure and the integrity of the photoreceptor mosaic. Invest Ophthalmol Vis Sci 53:8006-8015.

Chang B, Hawes NL, Hurd RE, Davisson MT, Nusinowitz S, Heckenlively JR (2002) Retinal degeneration mutants in the mouse. Vision Res 42:517-525.

Chen YY, Liu SL, Hu DP, Xing YQ, Shen Y (2014) N-methyl- N-nitrosourea-induced retinal degeneration in mice. Exp Eye Res 121:102-113.

Creel DJ (2019) Electroretinograms. Handb Clin Neurol 160:481-493.

Deng CL, Hu CB, Ling ST, Zhao N, Bao LH, Zhou F, Xiong YC, Chen T, Sui BD, Yu XR, Hu CH (2021) Photoreceptor protection by mesenchymal stem cell transplantation identifies exosomal MiR-21 as a therapeutic for retinal degeneration. Cell Death Differ 28:1041-1061.

Dias MF, Joo K, Kemp JA, Fialho SL, da Silva Cunha A, Jr., Woo SJ, Kwon YJ (2018) Molecular genetics and emerging therapies for retinitis pigmentosa: Basic research and clinical perspectives. Prog Retin Eye Res 63:107-131.

Emoto Y, Yoshizawa K, Uehara N, Kinoshita Y, Yuri T, Shikata N, Tsubura A (2013) Curcumin suppresses N-methyl-N-nitrosourea-induced photoreceptor apoptosis in Sprague-Dawley rats. In Vivo 27:583-590.

Fu YW, Peng YF, Huang XD, Yang Y, Huang L, Xi Y, Hu ZF, Lin S, So KF, Ren CR (2021) Lycium barbarum polysaccharide-glycoprotein preventative treatment ameliorates aversive. Neural Regen Res 16:543-549.

Hartong DT, Berson EL, Dryja TP (2006) Retinitis pigmentosa. Lancet 368:1795-1809.

Hayakawa R, Komoike K, Kawakami H, Morishima M, Shimizu K, Kitahara S, Fujieda H, Ezaki T (2020) Ultrastructural changes in the choriocapillaris of N-methyl-N-nitrosourea-induced retinal degeneration in C57BL/6 mice. Med Mol Morphol 53:198-209.

Huang Y, Zheng Y, Yang F, Feng Y, Xu K, Wu J, Qu S, Yu Z, Fan F, Huang L, Qin M, He Z, Nie K, So KF (2022) Lycium barbarum Glycopeptide prevents the development and progression of acute colitis by regulating the composition and diversity of the gut microbiota in mice. Front Cell Infect Microbiol 12:921075.

Kotliarova A, Sidorova YA (2021) Glial cell line-derived neurotrophic factor family ligands, players at the interface of neuroinflammation and neuroprotection: focus onto the glia. Front Cell Neurosci 15:679034.

Leinonen HO, Bull E, Fu Z (2023) Neural and Müller glial adaptation of the retina to photoreceptor degeneration. Neural Regen Res 18:701-707.

Liu F, Zhang J, Xiang Z, Xu D, So KF, Vardi N, Xu Y (2018) Lycium barbarum polysaccharides protect retina in rd1 mice during photoreceptor degeneration. Invest Ophthalmol Vis Sci 59:597-611.

Liu XB, Liu F, Liang YY, Yin G, Zhang HJ, Mi XS, Zhang ZJ, So KF, Li A, Xu Y (2021) Luteolin delays photoreceptor degeneration in a mouse model of retinitis pigmentosa. Neural Regen Res 16:2109-2120.

Livak KJ, Schmittgen TD (2001) Analysis of relative gene expression data using real-time quantitative PCR and the 2(-Delta Delta C(T)) Method. Methods 25:402-408.

Ma RL, Wan J, Yu A, She ZY, Wu GC, Zhang R (2006) Effects of acupuncture on N-methyl-N-nitrosourea-induced degeneration of the retina in rats. Zhenci Yanjiu 31:276-279.

Manthey AL, Chiu K, So KF (2017) Effects of Lycium barbarum on the visual system. Int Rev Neurobiol 135:1-27.

Massengill MT, Ahmed CM, Lewin AS, Ildefonso CJ (2018) Neuroinflammation in retinitis pigmentosa, diabetic retinopathy, and age-related macular degeneration: a minireview. Adv Exp Med Biol 1074:185-191.

Mi XS, Feng Q, Lo AC, Chang RC, Lin B, Chung SK, So KF (2012) Protection of retinal ganglion cells and retinal vasculature by Lycium barbarum polysaccharides in a mouse model of acute ocular hypertension. PLoS One 7:e45469.

Milla-Navarro S, Pazo-González M, Germain F, de la Villa P (2022) Phenotype characterization of a mice genetic model of absolute blindness. Int J Mol Sci 23:8152.

Moon CH, Cho H, Kim YK, Park TK (2017) Nestin expression in the adult mouse retina with pharmaceutically induced retinal degeneration. J Korean Med Sci 32:343-351.

Neelam K, Dey S, Sim R, Lee J, Au Eong KG (2021) Fructus lycii: a natural dietary supplement for amelioration of retinal diseases. Nutrients 13:246.

Silverman SM, Wong WT (2018) Microglia in the retina: roles in development, maturity, and disease. Annu Rev Vis Sci 4:45-77.

Slepko N, Levi G (1996) Progressive activation of adult microglial cells in vitro. Glia 16:241-246.

Song MK, Salam NK, Roufogalis BD, Huang TH (2011) Lycium barbarum (Goji Berry) extracts and its taurine component inhibit PPAR-γ-dependent gene transcription in human retinal pigment epithelial cells: possible implications for diabetic retinopathy treatment. Biochem Pharmacol 82:1209-1218.

Sun X, Shao H, Xiang K, Yan Y, Yu X, Li D, Wu W, Zhou L, So KF, Ren Y, Ramakrishna S, Li A, He L (2017) Poly(dopamine)-modified carbon nanotube multilayered film and its effects on macrophages. Carbon 113:176-191.

Tang L, Bao S, Du Y, Jiang Z, Wuliji AO, Ren X, Zhang C, Chu H, Kong L, Ma H (2018) Antioxidant effects of Lycium barbarum polysaccharides on photoreceptor degeneration in the light-exposed mouse retina. Biomed Pharmacother 103:829-837.

Tao Y, Chen T, Fang W, Peng G, Wang L, Qin L, Liu B, Fei Huang Y (2015) The temporal topography of the N-methyl-N-nitrosourea induced photoreceptor degeneration in mouse retina. Sci Rep 5:18612.

Tian GY, Wang C, Feng YC (1995) Isolation, purification and properties of LbGP and characterization of its glycan-peptide bond. Shengwu Huaxue yu Shengwu Wuli Xuebao 27:201-206.

Tsubura A, Lai YC, Miki H, Sasaki T, Uehara N, Yuri T, Yoshizawa K (2011) Review: Animal models of N-methyl-N-nitrosourea-induced mammary cancer and retinal degeneration with special emphasis on therapeutic trials. In Vivo 25:11-22.

Verbakel SK, van Huet RAC, Boon CJF, den Hollander AI, Collin RWJ, Klaver CCW, Hoyng CB, Roepman R, Klevering BJ (2018) Non-syndromic retinitis pigmentosa. Prog Retin Eye Res 66:157-186.

Wang AL, Knight DK, Vu TT, Mehta MC (2019) Retinitis pigmentosa: review of current treatment. Int Ophthalmol Clin 59:263-280.

Wang K, Xiao J, Peng B, Xing F, So KF, Tipoe GL, Lin B (2014) Retinal structure and function preservation by polysaccharides of wolfberry in a mouse model of retinal degeneration. Sci Rep 4:7601.

Wong WL, Su X, Li X, Cheung CM, Klein R, Cheng CY, Wong TY (2014) Global prevalence of age-related macular degeneration and disease burden projection for 2020 and 2040: a systematic review and meta-analysis. Lancet Glob Health 2:e106-116.

Wu Y (2022) Antioxidant effect of lycium barbarum glycopeptide preconditioningon retinal ischemia reperfusion injury in rats. Chengdu: Chengdu University of Traditional Chinese Medicine. 2022.

Xiang Z, Bao Y, Zhang J, Liu C, Xu D, Liu F, Chen H, He L, Ramakrishna S, Zhang Z, Vardi N, Xu Y (2018) Inhibition of non-NMDA ionotropic glutamate receptors delays the retinal degeneration in rd10 mouse. Neuropharmacology 139:137-149.

Xiong Y, Ji HP, Song WT, Yin YW, Xia CH, Xu B, Xu Y, Xia XB (2016) N-methyl-N-nitrosourea induces retinal degeneration in the rat via the inhibition of NF-κB activation. Cell Biochem Funct 34:588-596.

Yang J, Lin S, Hu S, Chen K, Deng X (2004) The toxic effect of N-methyl-N- nitrosourea on retina in rats. Yan Ke Xue Bao 20:249-254.

Yao Q, Yang Y, Lu X, Zhang Q, Luo M, Li PA, Pan Y (2018) Lycium barbarum polysaccharides improve retinopathy in diabetic Sprague-Dawley rats. Evid Based Complement Alternat Med 2018:7943212.

Yoshizawa K, Nambu H, Yang J, Oishi Y, Senzaki H, Shikata N, Miki H, Tsubura A (1999) Mechanisms of photoreceptor cell apoptosis induced by N-methyl-N-nitrosourea in Sprague-Dawley rats. Lab Invest 79:1359-1367.

Yuan LG, Deng HB, Chen LH, Li DD, He QY (2008) Reversal of apoptotic resistance by Lycium barbarum glycopeptide 3 in aged T cells. Biomed Environ Sci 21:212-217.

Yuge K, Nambu H, Senzaki H, Nakao I, Miki H, Uyama M, Tsubura A (1996) N-methyl-N-nitrosourea-induced photoreceptor apoptosis in the mouse retina. In Vivo 10:483-488.

Zhang HJ, Liu XB, Chen XM, Kong QH, Liu YS, So KF, Chen JS, Xu Y, Mi XS, Tang SB (2022a) Lutein delays photoreceptor degeneration in a mouse model of retinitis pigmentosa. Neural Regen Res 17:1596-1603.

Zhang J, Xu D, Ouyang H, Hu S, Li A, Luo H, Xu Y (2017) Neuroprotective effects of methyl 3,4 dihydroxybenzoate in a mouse model of retinitis pigmentosa. Exp Eye Res 162:86-96.

Zhang J, Li P, Zhao G, He S, Xu D, Jiang W, Peng Q, Li Z, Xie Z, Zhang H, Xu Y, Qi L (2022b) Mesenchymal stem cell-derived extracellular vesicles protect retina in a mouse model of retinitis pigmentosa by anti-inflammation through miR-146a-Nr4a3 axis. Stem Cell Res Ther 13:394.

Zhang YK, Wang J, Liu L, Chang RC, So KF, Ju G (2013) The effect of Lycium barbarum on spinal cord injury, particularly its relationship with M1 and M2 macrophage in rats. BMC Complement Altern Med 13:67.

Zheng HL, Li MT, Zhou T, Wang YY, Shang EX, Hua YQ, Duan JA, Zhu Y (2023) Protective effects of Lycium barbarum L. berry extracts against oxidative stress-induced damage of the retina of aging mouse and ARPE-19 cells. Food Funct 14:399-412.

Zhou X, Zhang Z, Shi H, Liu Q, Chang Y, Feng W, Zhu S, Sun S (2022) Effects of Lycium barbarum glycopeptide on renal and testicular injury induced by di(2-ethylhexyl) phthalate. Cell Stress Chaperones 27:257-271.

Zhu Y, Zhao Q, Gao H, Peng X, Wen Y, Dai G (2016) Lycium barbarum polysaccharides attenuates N-methy-N-nitrosourea-induced photoreceptor cell apoptosis in rats through regulation of poly (ADP-ribose) polymerase and caspase expression. J Ethnopharmacol 191:125-134.

Additional Figure 1 The retinal light responses of photoreceptor degenerated mice.
(A) Representative electroretinogram traces of each group to flash at photopic 10.0 cd/m^2. (B) Peak amplitudes (amp) of the a- and b-waves under photopic conditions for each flash intensity. (C) Latency of the a- and b-waves. Data are presented as mean ± SEM (Con: n = 8, MNU: n = 8, LbGP: n = 10). *P < 0.05, **P < 0.01 (one-way analysis of variance followed by Tukey's *post hoc* test). Con: C57BL/6J mice; LbGP: N-methyl-N-nitrosourea-injured mice with *Lycium barbarum* glycopeptide treatment; MNU: N-methyl-N-nitrosourea-injured mice without treatment.